Analysis of the particulate emissions and combustion performance of a direct injection spark ignition engine using hydrogen and gasoline mixtures

Analysis of the Particulate Emissions and Combustion Performance of a Direct Injection Spark Ignition Engine Using Hydrogen and Gasoline Mixtures

Huayong Zhao [a], Richard Stone [a,*], Lei Zhou [a,b]

[a] *Department of Engineering Science, University of Oxford, Parks Road, Oxford, U.K., OX1 3PJ*

[b] *School of Mechanical and Vehicular Engineering, Beijing Institute of Technology,*

Beijing 100081, P.R. China

Abstract

Three different fractions (2%, 5%, and 10% of stoichiometric, or 2.38%, 5.92%, and 11.73% by energy fraction) of hydrogen were aspirated into a gasoline direct injection engine under two different load conditions. The base fuel was 65% iso-octane, and 35% toluene by volume fraction. Ignition sweeps were conducted for each operation point. The pressure traces were recorded for further analysis, and the particulate emission size distributions were measured using a Cambustion DMS500. The results indicated a more stable and faster combustion as more hydrogen was blended. Meanwhile, a substantial reduction in particulate emissions was found at the low load condition (more than 95% reduction either in terms of number concentration or mass concentration when blending 10% hydrogen). Some variation in the results occurred at the high load condition, but the particulate emissions were reduced in most cases, especially for nucleation mode particulate matter. Retarding the ignition timing generally reduced the particulate emissions. An engine model was constructed using the Ricardo WAVE package to assist in understanding the data. The simulation reported a higher residual gas fraction at low load, which explained the higher level of cycle-by-cycle variation at the low load.

Keywords: hydrogen; gasoline direct injection engine; combustion; particulate emissions

1. Introduction

As the most recent generation of SI engine, Gasoline Direct Injection (GDI) engines have the potential to achieve a comparable fuel economy to diesel engine and with a higher power output compared to conventional port fuel injection SI engines. Meanwhile, the ever increasingly stringent emissions legislation (Table 1) has brought some new challenges for GDI engines.

The legislation for Particulate Matter is particularly challenging, both in terms of measurements and in ensuring conformity to legislation. PM emissions are one of the disadvantages of the GDI engine due to the reduced time for fuel-air mixing. The restriction in PM emission applied to diesel engine ($6.0*10^{11}$/km) might also be applied to GDI engines in the near future. In addition, PM has been found to have adverse effects on human health (Donaldson and MacNee, 1998, Pandya et al., 2002), especially for the smaller particles, since they have a higher deposition efficiency in the human respiratory system. SI engines have been found to be the main sources for fine or ultrafine particules (Kittelson, 1998). From diesel engine research, it is known that blending hydrogen reduces PM emissions, but no such tests appear to have been reported for GDI engines.

Hydrogen has many attractive intrinsic properties that make it a promising fuel. The lower minimum ignition energy of hydrogen ensures a more stable ignition and eases cold start engine operation, but raises the danger of abnormal combustion. Its high laminar burning velocity (around five times faster than that of gasoline) is expected to increase the indicated efficiency and reduce the cycle-to-cycle variations in combustion. The higher diffusion coefficient of hydrogen may enhance the mixing process, which also can increase the engine efficiency and help to produce less soot and unburned hydrocarbons. Hydrogen also has a smaller quenching distance compared to gasoline, so that the flame can travel further into crevices to ensure more complete combustion. Moreover, adding hydrogen is expected to extend the lean limit due to its lower flammability limit in air. However, the lower net energy density of hydrogen compared with gasoline for a unit volume of stoichiometric mixture with air may reduce the power output. Adding hydrogen also produces a higher adiabatic flame temperature in air, which raises concerns over NO_x emissions.

2. Literature Reviews

Many researchers have investigated the effect of adding hydrogen in a gasoline engine in various ways. Conte and Boulouchos (2008) investigated hydrogen-enhanced gasoline stratified charge combustion in GDI engines. They reported a more efficient and stable combustion when adding hydrogen. Moreover, by considering the energy used to produce hydrogen on-board by using a gasoline reformer, they believed the efficiency gains for adding hydrogen were large enough to compensate for the energy used in producing the hydrogen. As for the emissions, higher NOx emissions were reported. However, by increasing the EGR percentage and delaying the ignition timing at low load or by delaying the ignition timing solely at high load, they achieved a lower NO_x/IMEP ratio compared with operation on pure gasoline and a normal EGR percentage. The unburned hydrocarbons, according to their experimental data, were reduced when adding hydrogen. They suggested that this was due to better combustion stability and having a lower fraction of gasoline in the fuel mixture.

Andrea et al. (2004) studied the combustion and emission characteristics of a SI engine when it operated with hydrogen-blended gasoline at lean conditions. They suggested a critical equivalence ratio (λ) of 1.18. When the engine is running at $\lambda < 1.18$, there was no big difference in the torque output and burn rate when adding hydrogen. When $\lambda > 1.18$, torque increased and the burn duration was reduced. As for the emissions, they only investigated the NO emission. When $\lambda = 1$, they found very little difference when adding hydrogen. But as $\lambda > 1.25$, adding hydrogen increased the NO emissions; they attributed this effect to a higher flame temperature. By considering the cost of on-board electrolysis as a method to produce hydrogen, they concluded that the energy gain by adding hydrogen into the gasoline was not sufficient to compensate for the energy used to produce the hydrogen.

As on-board gasoline reforming is becoming a more popular way to produce hydrogen, Suzuki and Sakurai (2006) investigated the combustion characteristics of a SI engine fuelled by gasoline and hydrogen or a simulated hydrogen rich reformer gas (Steam Reforming gas and Autothermal Reforming gas) mixture. They found that the MBT points were retarded significantly as the hydrogen fraction was increased. In addition, the indicated thermal efficiency was found to be higher when the gasoline was blended with hydrogen than when it was blended with steam reforming gases or auto-thermal reforming gases at low load. But at high load, no big difference was reported when various gaseous fuels were blended. Jamal et al. (1996) investigated the effectiveness of on-board exhaust gas reforming of gasoline at moderate reformer temperature (600 and 650 °C). According to their experiments, adding reformed fuel in a gasoline operated engine could decrease the UBHC and NOx emissions, increase the overall engine efficiency and smooth the engine operation. However, the hydrogen fractions (up to 4.81% by molar concentration) obtained by exhaust gas reforming at these temperatures are much lower than that predicted by calculation based on Gibbs function minimisation. A new on-board exhaust gas reforming technology by using integrated reformer and TWC (Three Way Catalytic converter), which could produce a reformed fuel with higher energy content (up to 11% H_2 by volume fraction), was introduced by Ashur et al. (2007). An overview of hydrogen production technologies was provided by Holladay et al. (2009), and a review on on-board generation of hydrogen-rich gaseous fuels was given by Yamal and Wyszynski (1993).

The effect of hydrogen addition on knock behaviour is reported by Shinagawa et al. (2004). They found that hydrogen addition can reduce the margin between the ignition timing which caused knock and that for MBT. In addition, the knock behaviour was found to be greatly affected by the distribution of hydrogen, which can be changed by injection direction and injection timings. Knock-free operation at MBT was reported when the hydrogen was unevenly distributed, not only near the wall, but also near the spark plug at 10°BTDC. They concluded that since hydrogen can reduce the combustion period and inhibit fuel decomposition and hydroxyl radical production, then knock can be avoided by adding hydrogen.

Though the effect of adding hydrogen in a gasoline operated engine has been studied by numerous researchers, few experiments have been done using GDI engines. Moreover, no data was found for the PM emissions when hydrogen is blended into a GDI engine. This paper will discuss the combustion and emission characteristics of a hydrogen-aspirated GDI engine in great detail, especially the PM emissions.

3. Experiment Setup and Tests Conditions

3.1 Experimental Setup

All experiments were with an Optical Access Engine, with the specification summarized in Table 2.

A schematic picture of the overall set-up is shown in Fig.1. The fraction of hydrogen is controlled by a mass flow controller, which is carefully calibrated by using air and a positive displacement flow meter. Knowledge of the density

and specific heat capacities was used to convert the calibration from air to hydrogen. The base fuel (65% iso-octane and 35% toluene by volume fraction) has an aromatic content that matches the upper limit for European gasoline.

The intake air flow rate was measured with a positive displacement flow meter that gave a TTL signal with frequency which is proportional to the flow rate. A frequency to voltage converter provides an analogue output which was used as an input to the interface control box that sent a demand value to the hydrogen mass flow controller (See Fig.1). According to the energy calculation and calibration data, the relationship between hydrogen flow rate and air flow rate for *x* % of stoichiometric hydrogen fraction is:

$$V'_{H2}/V'_{air} = 0.0444 * x/C1 \qquad \text{Eq. (1)}$$

*C*1 is the gain value (2*, 5*, and 10*) from the interface box. The hydrogen fraction was controlled by adjusting the value of a ten-turn potentiometer.

The overall mixture was measured by a lambda sensor in the exhaust gas, and when hydrogen was added the quantity (*x*) was defined in terms of a percentage of the stoichiometric mixture. This is best illustrated by an example – 10% hydrogen is equivalent to saying that 10% of the air flow was mixed with a stoichiometric mixture of hydrogen. The overall mixture strength was then adjusted by control of the injection duration of the liquid fuel.The Engine Timing Control System (ETCS) was used to set the ignition timing, injection timing, injection duration etc; it also supervised the Data Acquisition (DAQ) system. The DAQ system consisted of a high speed data acquisition (HDAQ) system and a low speed data acquisition (LDAQ) system. The HDAQ system used a National Instruments PCI-MIO-16E-1 data acquisition card with 12-bit resolution. Its sampling rate was one sample per crank angle, or 9 kHz when the engine is operated at 1500 rpm. The HDAQ system was for recording high frequency signals, such as the pressure trace, or the crank signal. A National Instruments® PCI-6024E DAQ card with 12-bit resolution was used in the LDAQ system. Its sampling rate was about 0.5 Hz. The relatively low frequency signals, such as temperatures, equivalence ratio, or the torque were logged into the LDAQ system. The cylinder pressure data from the DAQ system was further analyzed by various Matlab codes to calculate the burn rate or the cumulative mass fraction burn, using the approach devised by Rassweiler and Withrow (1938). The Particulate Matter (PM) number distributions were measured by a Cambustion DMS500 Differential Mobility Spectrometer, which enabled a real-time measurement of PM ranging from 4nm to 1000 nm. The mass distributions were calculated with the assumption that the particules are spherical and the density is only a function of the diameter. The empirical equation used to calculate the mass (*m, kg*) is:

$$m = 1.72 * 10^{-24} * D_p^{2.65} \qquad \text{Eq. (2)}$$

Where D_p (nm) is the diameter of the particle (Symonds et al., 2008).

Finally, the data were analyzed and plotted by using various codes written in Matlab. The legends on all plots are in the format *'fuel-lambda-notes'*. For example, *'Base-0.9'* represents the raw data points from the test using base fuel at lambda equal to 0.9; *'H2-0.9-fitting'* represents the fitting curve for the data from the test using base fuel with 2% of a stoichiometric mixture being hydrogen and a lambda equal to 0.9.

3.2 Tests Conditions

Tests were operated under two load conditions as summarized as in Table 3. The rich of stoichiometric mixture was used to investigate what might happen at wide open throttle, when operation is in a regime that does not form part of a drive cycle. The rich mixture increases the torque output and prevents catalyst overheating at high engine speeds.

Filter samples for richer mixture were taken for later analysis of the particulate matter composition. The valve timing in these experiments is different from those of traditional engines. Because of the valve overlap, the late inlet valve opening leads to a high level of hot residuals that will reduce the engine-out NOx emissions, but more significantly it is used to reduce the throttling loss at part load. This is comparable to exhaust gas recirculation, but is controlled by the valve event control system. This avoids the need for external hardware and provides residuals that are hot, so that mixture preparation is assisted. As the residuals are hot they displace more air (so the throttling loss is reduced more) and the higher mixture temperature permits a higher level of residuals too.

4. Results and Discussion

4.1 Combustion Analysis

To find the effect of blending hydrogen on the engine power output and the Minimum (ignition) advance for Best Torque (MBT) ignition timing, the net Indicated Mean Effective Pressures (IMEPn) were plotted *versus* ignition timing as shown in Fig. 2. For both load conditions, the IMEPn for the richer mixture ($\lambda = 0.9$) is higher than that for the stoichiometric mixture. This is due to the better usage of oxygen in rich mixture combustion. As for the effect of blending hydrogen on the maximum IMEPn for different fuels, the trend is less obvious. When blending hydrogen, part of the incoming air will be replaced by the hydrogen, so this reduces the IMEPn. Although hydrogen has a much higher calorific value than gasoline its stoichiometric air fuel ratio is about 34:1, and this decreases the calorific value of a stoichiometric mixture per mole of mixture. The overall result is that blending hydrogen will reduced the energy content of the mixture trapped in the cylinder (see Fig. 3). However, the faster combustion with hydrogen will mean an increase in IMEP, so that the reduction in IMEP is less than the theoretical prediction.

The MBT ignition timings were found by looking at the maxima of the second order polynomial fits to the experimental IMEPn data; the results are shown in Table 4. The general behaviour is that blending hydrogen retards the MBT ignition timing toward tdc. This is because the higher burn rate (when blending hydrogen) leads to a much higher cylinder pressure during the compression stroke, so that the work gain during the expansion stroke is not enough to compensate for the work loss during the compression stroke. When this occurs, the ignition timing should be retarded to give a lower cylinder pressure. In addition, the effects of hydrogen blending are less significant for richer mixtures than for a stoichiometric mixture. This is because rich mixtures are inherently faster burning, so hydrogen blending has less effect on reducing the burn duration with richer mixtures.

The cycle-by-cycle variation of the IMEP is another important parameter for the engine's smooth operation. It is indicated by the coefficient of variation (CoV). Plots of the CoV of IMEPn are shown in Fig.4. For both load conditions, blending hydrogen improves the combustion stability significantly, especially at the low load/stoichiometric condition. At low load, the engine experience poor combustion stability due to the high percentage of residual gases trapped as suggested by the simulation results (the CoV for a stoichiometric mixture is 16%, which would be unacceptable in normal operation). From the simulation, the residual gas fraction at low load is above 18.5% over the whole range of ignition timings; at high load, it is about 16%. When blending 5% of hydrogen at low load, the CoV can be reduced to well below 10%, and blending 10% of hydrogen can further reduce the CoV below 5%. Moreover, most of the minimum CoV_{IMEP} occurs around the MBT ignition timings. This is in part because the mean values of IMEP are highest, but it is also because combustion in the MBT ignition region is the most stable.

Blending hydrogen also speeds up the combustion because of the higher flame speed of hydrogen, as shown in Fig.5. The higher flame speed of hydrogen is believed to be the main reason. By looking at the difference between the 0-80% mfb (Mass Faction burned) curve and the 0-10% curve, except for extremely late ignition timings, the 0-10% mfb duration is about equal to the 10-80% mfb duration, and the burn duration for the richer mixture is shorter than that for the stoichiometric mixture. Moreover, the effect of blending hydrogen is more significant for the stoichiometric mixtures than the richer mixtures since the burn rate is inherently higher for the richer mixtures.

4.2 Particulate Matter (PM) Emissions

The PM emission reduction factor (PMRF) of number or mass (calculated) is used to quantify the effect of blending hydrogen, and it is defined as:

$$\text{PMRF (Number/Mass)} = \frac{\text{PM emissions (total number/mass) for the base fuel}}{\text{PM emissions (total number/mass) for hydrogen-blended fuel}} \qquad \text{Eq. (3)}$$

Since PM with diameters less than 23 nm are not taken into account by the European emission legislation, they were excluded when calculating the PMRF.

4.2.1 Low Load Condition

As can be seen from Fig.6, blending hydrogen can reduce the PM emissions substantially at the low load condition. For the stoichiometric mixture, just 5% of stoichiometric hydrogen blending can reduce the total PM number and total PM mass by up to 90% (PMRF = 10), and 10% of hydrogen can further reduce the total number up to 97% (PMRF = 30), and reduce the total mass up to 95% (PMRF = 20). When compared at the MBT ignition timings, the PMRF is even higher. For the rich mixture, the hydrogen blending leads to a more remarkable reduction in total PM number. Hydrogen blending of 5% reduces PM by up to 97% (PMRF = 30). But the total PM mass is reduced by less than 90% (PMRF = 10). This is because although the total number concentration is dominated by nucleation mode PM (diameter less than 100 nm), the mass is dominated by the accumulation mode PM (diameter ranges from 100 to 1000 nm), especially the

PM with diameter ranges from 100 to 500 nm since the number of particules larger than 500 nm is very small. Blending hydrogen reduces the nucleation mode PM notably, but has less effect on the accumulation mode PM. This can be seen from Fig.7.

Since it is always desirable to operate the engine in the MBT ignition timing region, the PM emissions at MBT ignition timings are plotted separately, as in Fig.8, for comparison. It can be clearly seen that hydrogen blending reduces both the PM number concentration and mass concentration notably: 10 % hydrogen blending reduces the total number and mass concentration by more than 95% for the stoichiometric mixture, and for the richer mixture, the number concentration is reduced by 97%, and the mass concentration is reduced by around 92%. As for particulate matter smaller than 23 nm, they are important to the number concentration, but of negligible importance to the mass concentration.

The detailed PM number and mass distributions are plotted in Fig.9. It can be clearly seen that PM larger than 23nm are effectively reduced over the whole size range as more hydrogen is blended. But for the PM smaller than 23nm, some variation in the results is found. Since smaller particles tend to have charges, the accuracy of the data in this range may not be as good as in other ranges, and this has the potential to cause these variations. Furthermore, a slight change in the sampling temperature and dilution ratio can have a large effect on the number of sub-23 nm particles, which is presumably one of reasons that they are excluded in the EU legislation.

From the above data, it can be safely concluded that blending hydrogen can reduce the PM emissions remarkably at low load conditions for both the stoichiometric mixture and a richer mixture. This is partly because the high diffusion coefficient of hydrogen improves the mixing process. In addition, the high flame speed and smaller quenching distance of hydrogen results in a more complete combustion, which reduces the organic PM. In addition, blending hydrogen reduces the amount of available hydrocarbons, which would lead to a lower PM emission level. Another interesting phenomena is that blending hydrogen reduces the nucleation mode particles (below 100 nm) more notably than the accumulation mode particles. This might be due to the direct chemically inhibiting effect of hydrogen blending in the formation of nucleation mode particles, as proposed by Guo et al. (2006). The nucleation mode particulate matter are formed by the process of inception and surface growth. It is widely accepted that the polycyclic aromatic hydrocarbons (PAH) develop into soot particle nuclei when their structures reach a large enough size. The key reactions for the growth of aromatic rings from benzene are known as HACA (Hydrogen Abstraction Carbon Addition):

$$A_i + H \leftrightarrow A_i^* + H_2 \quad \text{(R1)}$$

$$A_i^* + C_2H_2 \leftrightarrow A_iC_2H_2^* \quad \text{(R2)}$$

$$A_iC_2H_2^* + C_2H_2 \rightarrow A_{i+1} + H \quad \text{(R3)}$$

Where A_i represents i-ring aromatics and * indicates the active sites.
The blended molecular hydrogen will increase the reverse hydrogen abstraction reaction (R1) rate so as to inhibit the growth of PAH. As for the surface growth, two key reactions in the HACA surface reactions are:

$$(C_{soot} - H) + H \leftrightarrow C_{soot}^* + H_2 \quad \text{(R4)}$$

$$C_{soot}^* + C_2H_2 \rightarrow (C_{soot} - H) + H \quad \text{(R5)}$$

Blending molecular hydrogen will promote the reverse H-abstraction reaction (R4) and reduce the concentration of atomic hydrogen due to preferential diffusion of hydrogen, Guo et al. (2006).

4.2.2 High Load Condition

For the rich mixture, blending 10% hydrogen leads to around an 85% reduction in the total PM number concentration and a 17% reduction in the total PM mass concentration, as in Fig.10. At the MBT ignition timing, blending 10% hydrogen reduces the total PM number by 93%, and the total PM mass by 33%, as in Fig.11. Though the effect is not as remarkable as at the low load condition, considering the much higher emission level, the effect is none the less significant. However, for the stoichiometric mixture, blending hydrogen does not affect the total PM number concentration much, but increases the total PM mass concentration slightly. Blending hydrogen does reduce the number of smaller particles, but it also encourages the formation of larger particles. Fig.12 shows the detailed number and mass distribution at the MBT ignition timings. For GDI engines there is more concern over meeting the legislation for PM number rather than mass.

As can be seen in Fig.11, for the stoichiometric mixture, blending hydrogen only reduces the PM smaller than 23 nm. This maybe because blending hydrogen speeds up the combustion significantly, so that the post-flame oxidation temperature decreases due to the large heat transfer coefficient in the optical engine. In addition, the higher cylinder pressure when blending hydrogen will force more charge to flow into the crevices so that more fuel can escape the main combustion phase, and the unburned fuel finally experience gas-to-particle conversion to form particulate emissions.

From the discussion above, it can be seen that blending hydrogen reduces the PM emission level more significantly at low load than at high load. A possible reason is that different pyrolytic reactions (fragmentation, polymerisation and

dehydrogenation) will proceed to form soot only when the cylinder temperature is high enough; otherwise, soot precursors alone are formed and emitted as organic PM (Akihama et al., 2001), the flame temperature at high load is high enough for pyrolytic reactions when blending hydrogen, and this will promote the production of soot nuclei. The increase in soot nuclei facilitates the formation of larger particles due to a more active agglomeration process. However, the critical temperature for pyrolytic reaction is seldom reported so more research is needed to validate this explanation.

5. Conclusions

Three different fractions of hydrogen were aspirated into a spray guided direct injection engine to replace some gasoline at two load conditions for a stoichiometric and rich mixture. The effect on combustion and particulate emissions characteristics are summarized as follows:

1. Blending hydrogen will reduce the energy content of the mixture trapped in the cylinder, thereby reducing the IMEP. However, the faster combustion with hydrogen will mean the reduction in IMEP is less than the simple theoretical prediction based on the energy of the trapped charge.

2. The MBT ignition timing is retarded towards TDC when hydrogen is blended.

3. The combustion stability is improved greatly as more hydrogen is blended at both load conditions. Using 5% of hydrogen can reduce the CoV_{IMEP} well below 10% in most cases; 10% of hydrogen can further reduce it below 5% at low load. However, due to the high residual gas level, the CoV_{IMEP} for a stoichiometric mixture when using the base fuel is unacceptably high at low load. At high load, 5% of hydrogen can assure a very smooth operation since the CoV_{IMEP} is well below 5% in most cases.

4. Blending hydrogen speeds up the combustion because of the higher burning velocity of. This effect is more notable at low load and for the stoichiometric mixture as these have inherently slower combustion.

5. At high load, blending hydrogen reduces the amount of smaller particles, but encourages the formation of accumulation mode particles. For the richer mixture, 10% hydrogen blending leads to around an 85% reduction of total PM number concentration and a reduction of the total PM mass concentration by 17%. But for stoichiometric mixture, blending hydrogen has a slightly negative effect on PM emissions in terms of total mass concentration.

6. With the stoichiometric mixture at low load, 5% of stoichiometric hydrogen blending can reduce the total PM number and total PM mass by up to 90% (PMRF = 10), and 10% of hydrogen can further reduce the total number by up to 97% (PMRF = 30), and reduce the total mass by up to 95% (PMRF = 20). When compared at the MBT ignition timings, the PMRF is even higher; for the richer mixture at low load, the hydrogen blending leads to a more remarkable reduction in total PM number. Hydrogen blending of 5% reduces PM by up to 97% (PMRF = 30). But the total PM mass is reduced by less than 90% (PMRF = 10).

Acknowledgement

We would like to thank Longfei Chen and Michael Braisher, for their kind help with the engine tests and to Ashok Bhattacharya for suggesting the experiments. Acknowledgement is also given to Jaguar Cars for support of the experiments.

Nomenclature and Abbreviations

AFR	Air Flow Rate
AFM	Air Flow Meter
BMBT	Before MBT ignition timing
CoV	Coefficient of Variation
ETCS	Engine Timing Control System
FID	Flame Ionization Detector
GDI	Gasoline Direct Injection
HACA	Hydrogen Abstraction Carbon Addition
HDAQ	High speed Data Acquisition
IMEPn	net Indicated Mean Effective Pressure
LCV	Lower Calorific Value
LDAQ	Low speed Data Acquisition
LEVC	Late Exhaust Valve Closure

LIVO	Late Intake Valve Opening
mfb	mass fraction burned
MBT	Minimum (Ignition) advance for Best Torque
MFC	Mass Flow Controller
PAH	Polycyclic Aromatic Hydrocarbons
PM	Particulate Mater
PMRF	Particulate Matter Reduction Factor
TDC	Top Dead CentreTWC Three Way Catalytic converter

References

Akihama, K., Takatori, Y., Inagaki, S., and Dean, A.M., 2001. Mechanism of the Smokeless Rich Diesel Combustion by Reducing Temperature. SAE Technical, 2001-01-0655.

Andrea, T.D., Henshaw, P.F., Ting, D. S-K., and Sobiesiak, A., 2003. Investigating Combustion Enhancement and Emissions Reduction with the Addition of $2H_2 + O_2$ to a SI Engine. SAE International, 2003-32-0011.

Andrea, T.D., Henshaw, P.F., and Ting, D.S-K., 2004. The Addition of Hydrogen to a Gasoline-fuelled Engine. International Journal of Hydrogen Energy, 29, 1541-1552.

Ashur, M., Misztal, J., Wyszynski, Tsolakis, A., Xu, H. M., Qiao, J., and Golunski, S., 2007. Onboard Exhaust Gas Reforming of Gasoline Using Integrated Reformer and TWC. SAE International, 2007-24-0078.

Conte, E., and Boulouchos, K., 2008. Hydrogen-enhanced Gasoline Stratified Combustion in SI-DI Engines. Journal of Engineering for Gas Turbines and Power, 130.

Donaldson, K., and MacNee, W., 1998. The Mechanism of Lung Injury Caused by PM_{10}. Air Pollution and Health.

EU Regulation EC/715/2007, 207

Guo, H., Liu, F., Smallwood, G. J., and Gulder, O. L., 2006. Numerical Study on the influence of hydrogen addition on soot formation in a laminar ethylene-air diffusion flame. Combustion and Flame, 145, 324-338.

Holladay, J. D., Hu, J., King, D. L., and Wang Y., 2009. An Overview of Hydrogen Production Technologies. Catalysis Today, 139, 244-260.

Jamal, Y., and Wyszynski, M. L., 1994. On-board Generation of Hydrogen-rich Gaseous Fuels - A Review. International Journal of Hydrogen Energy, 7, 557-572.

Jamal, Y., Wagner, T., and Wyszynski, M. L., 1996. Exhaust Gas Reforming of Gasoline at Moderate Temperatures. International Journal of Hydrogen Energy, 21, 507-519.

Kittelson, D.B., 1998. Engines and Nanoparticles: A Review. J. Aerosol. Sci. 29, 575-588.

Pandya, R.J., Solomon, G., Kinner, A., and Balmes, J.R., 2002. Diesel Exhaust and Ashma: Hypotheses and Molecular mechanisms of Action. Environmental Health Perspectives, 110, 103-112.

Rassweiler, G.M., and Withrow, L., 1938. Motion Pictures of Engine Flame Correlated with Pressure Cards. SAE paper 380139. (Reissued as SAE paper 800131in 1980)

Shingagawa, T., Okumura, T., Furuno, S., and Kim, K-O., 2004. Effects of Hydrogen Addition to SI Engine on Knock Behaviour. SAE International, 2004-01-1851.

Suzuki, T., and Sakurai, Y., 2006. Effect of Hydrogen Rich Gas and Gasoline Mixed Combustion on Spark Ignition Engine. SAE Technical Paper, 2006-01-3379.

Symonds, J., Price, P., Williams, P., and Stone, R., 2008. Density of Particles Emitted from a Gasoline Direct Injection Engine. 12th ETH Conference on Combustion Generated Nanoparticles, Zurich.

Tables:

Table 1 EU light duty tailpipe emissions requirements for gasoline passenger cars (EU Regulation EC/2007)

Effective Timing	CO (g/km)	THC (mg/km)	NMHC (mg/km)	NO_x (mg/km)	PM (mg/km)	PN (1/km)
EU3: 01/2000	2.30	200	n/a	150	n/a	n/a
EU4: 01/2005	1.00	100	n/a	80	n/a	n/a
EU5: 09/2009	1.00	100	68	60	n/a	n/a
EU5b: 10/2011	1.00	100	68	60	5.0/4.5	n/a
EU6: 09/2014	1.00	100	68	60	5.0/4.5	TBD**

Notes: CO: Carbon Monoxide; THC: Total Hydrocarbons; NMHC: Non Methane Hydrocarbons; NO_x: Oxides of Nitrogen; PM: Particulate Matter; PN: Particle Number. TBD: To Be Determined

Table 2 Specification of the Engine

Item	Characteristics
Engine Type	spray guided; direct injection
Bore*Stroke	89*90.3 mm
Compression Ratio	11.1
Cylinder Capacity	561.8cc
Injection Pressure	150 bar

Table 3 Engine Test Conditions

Parameters	Value 1 (Low load)		Value 2 (High Load)
IVO (ATDC)		33.5°	
IVC (ABDC)		61.5°	
EVO (BBDC)		20°	
EVC (ATDC)		50°	
Air Flow Rate	1.5 l/s		2.5 l/s
Ignition Timing (BTDC)	5 to 45°	with 5° increments	5 to 40°
Equivalence Ratio (λ)		0.9/1.0	
Injection Timing		280°btdc	
Engine Speed		1500 rpm	
Coolant / Inlet Air Temperature (°C)		80/40	

Notes: IVO: Intake Valve Open; IVC: Intake Valve Close; EVO: Exhaust Valve Open; EVC: Exhaust Valve Close.

Table 4 MBT Ignition timings (°btdc)

Load	λ	Base	H2	H5	H10
Low	0.9	40	39	35	32
	1	41	41	39	33
High	0.9	33	29	28	26
	1	36	33	28	24

Figures:

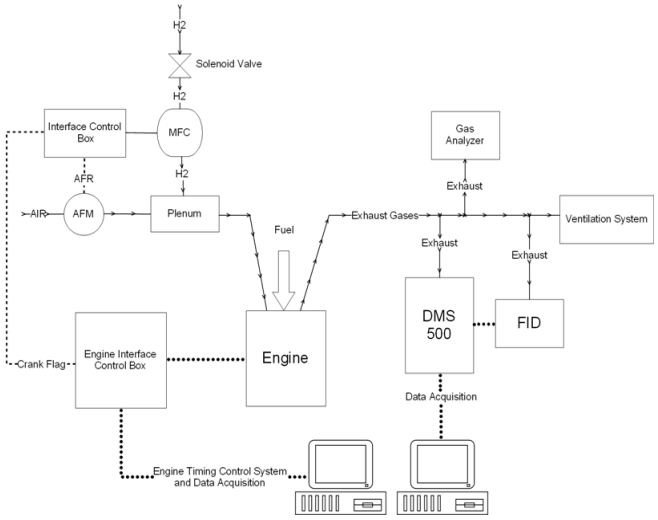

Fig.1 Experimental Set-up (MFC: Mass Flow Controller; AFM: Air Flow Meter; FID: Flame Ionization Detector; AFR: Air Flow Rate)

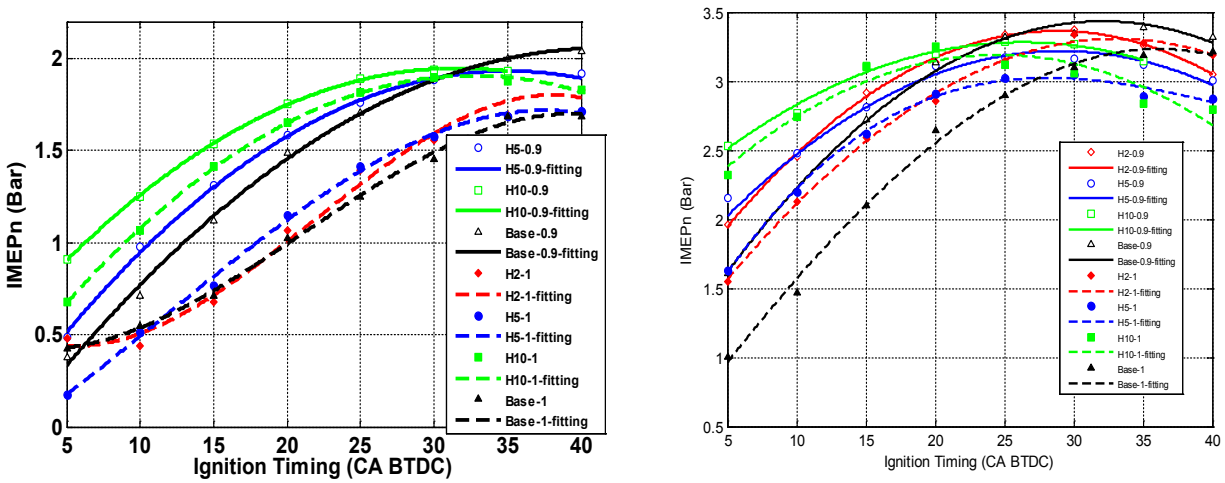

Fig. 2 IMEPn (net Indicated Mean Effective Pressure). Left is for low load, and right is for high load.

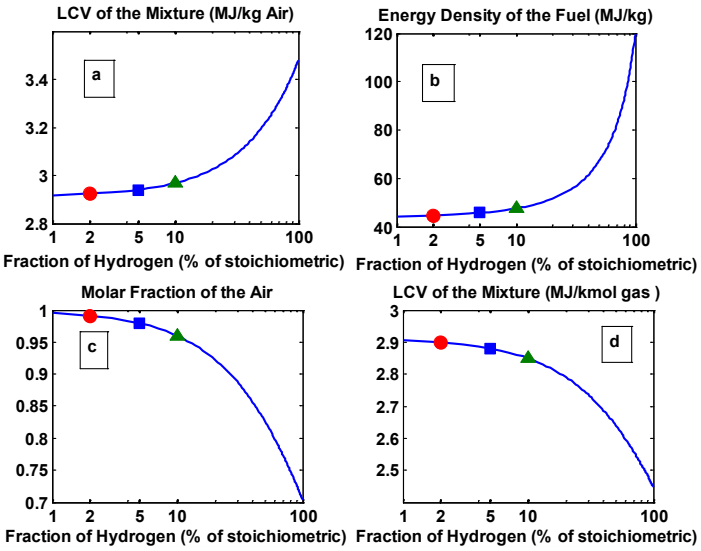

Fig. 3 (a) The Lower Calorific Value (LCV) of the mixture per kg of air; (b) Energy density of the fuel;
(c) Molar fraction of air in aspirated gas mixture; (d) The LCV of the mixture per kmol of aspirated gas mixture

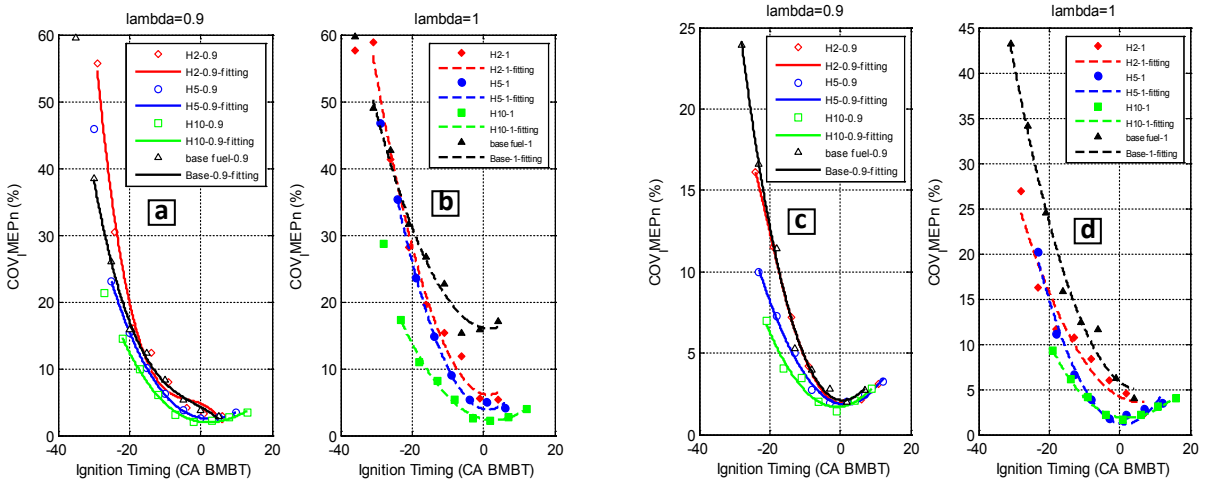

Fig. 4 CoV (Coefficient of Variation) of IMEPn, using MBT as the reference ignition timing for rich and stoichiometric mixtures; (a), (b) are for low load, and (c), (d) are for high load.

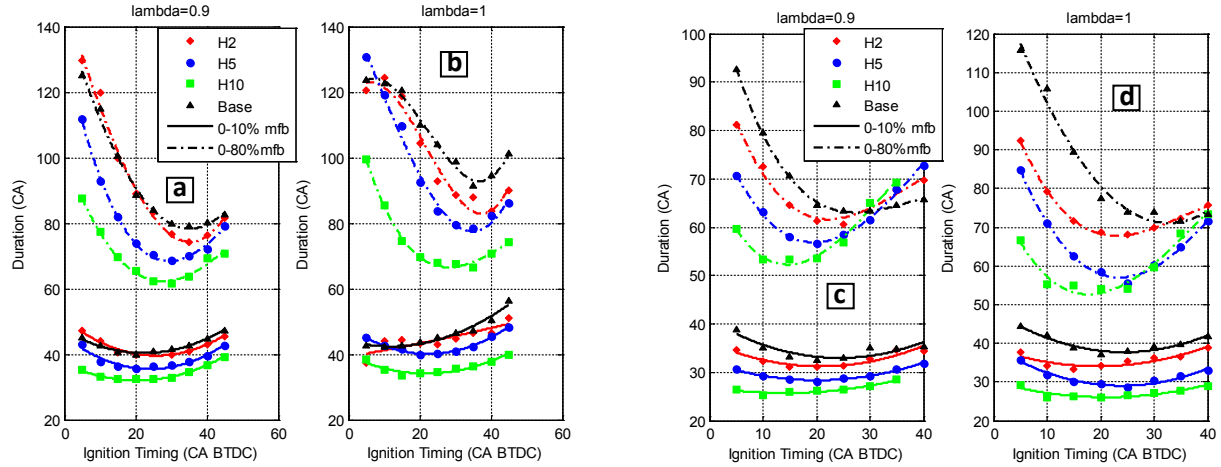

Fig. 5 Burn durations for rich and stoichiometric mixtures. (a), (b) are for low load, and (c), (d) are for high load.

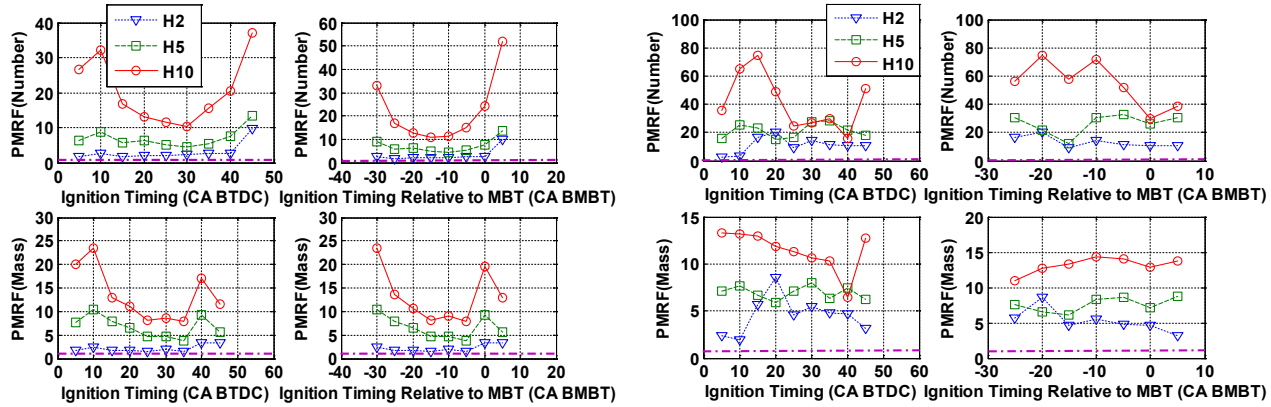

Fig. 6 PMRF (Particulate Matter Reduction Factor) at low load. Left is for λ = 1, and right is for λ = 0.9; the violet centreline represents PMRF = 1.

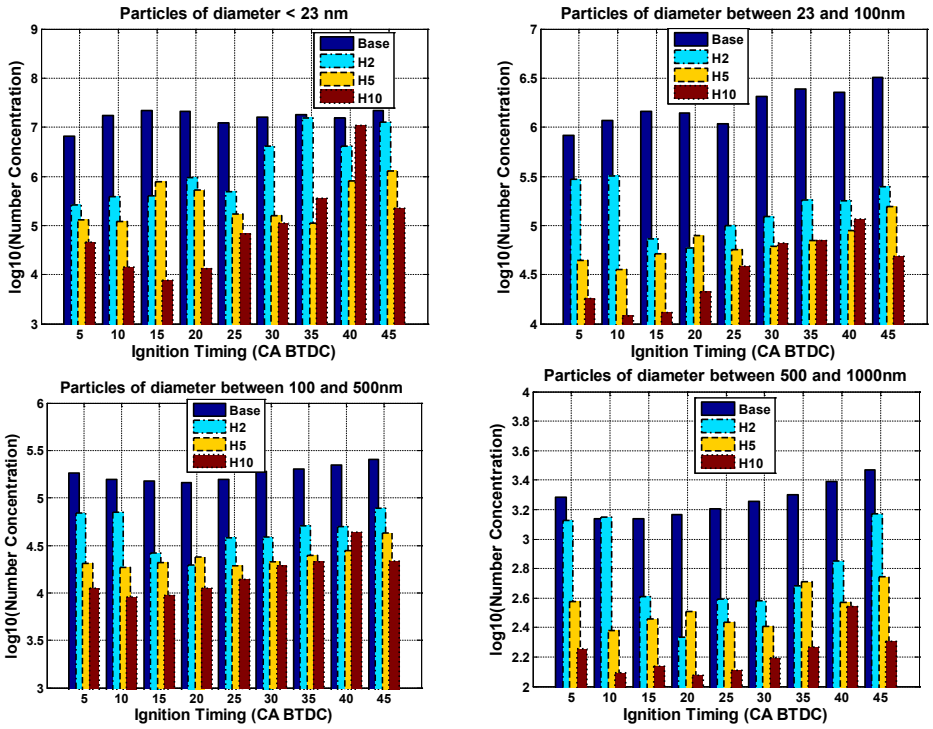

Fig. 7 Effect of blending hydrogen on the number concentration for different particle size ranges at λ = 0.9

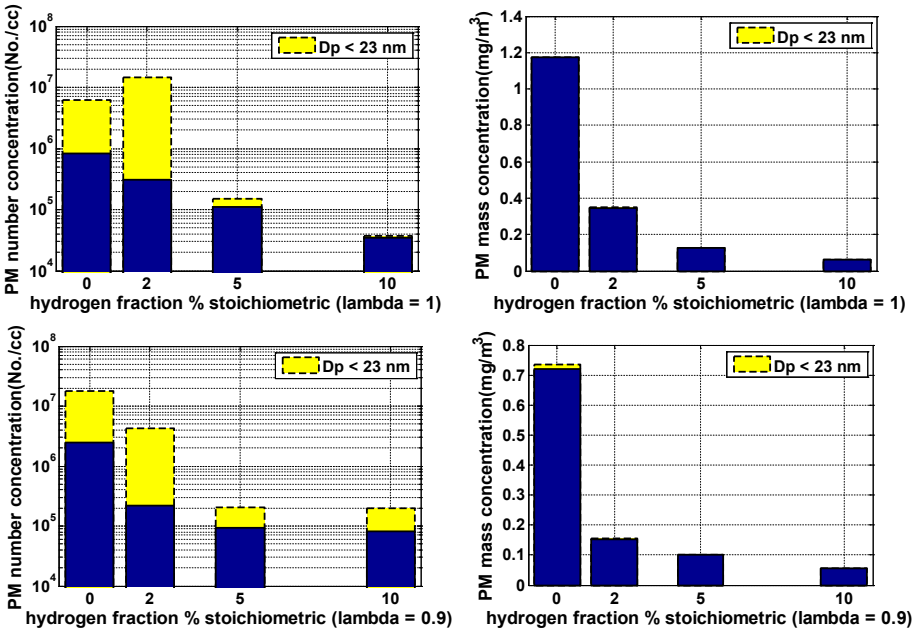

Fig. 8 PM number and mass at the MBT ignition timing at the low load. Upper two figures are for λ = 1, and the lower two are for λ = 0.9.; the area bounded by dashed line represents PM below 23nm, which is excluded in EU legislation.

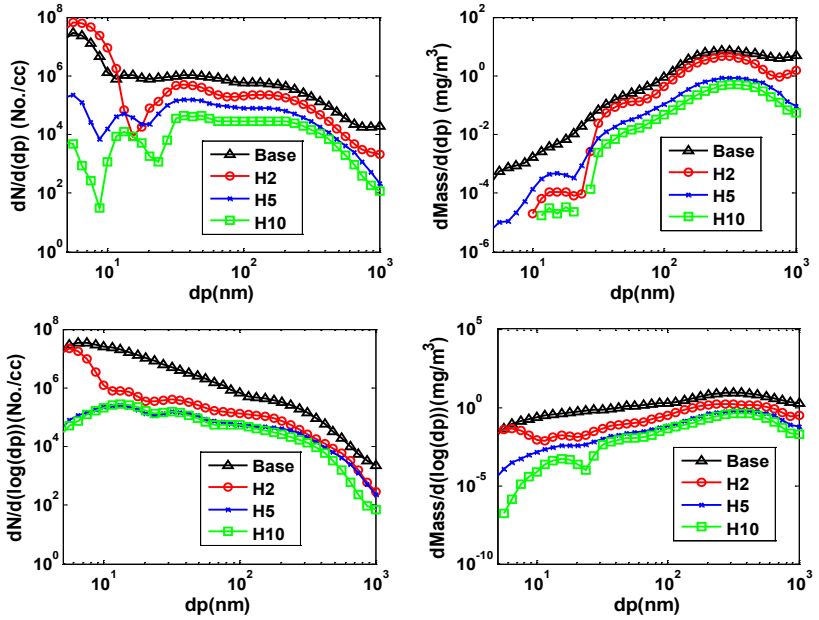

Fig. 9 PM number and mass distribution at MBT ignition timing and the low load. Upper two figures are for λ = 1, and the lower two are for λ = 0.9.

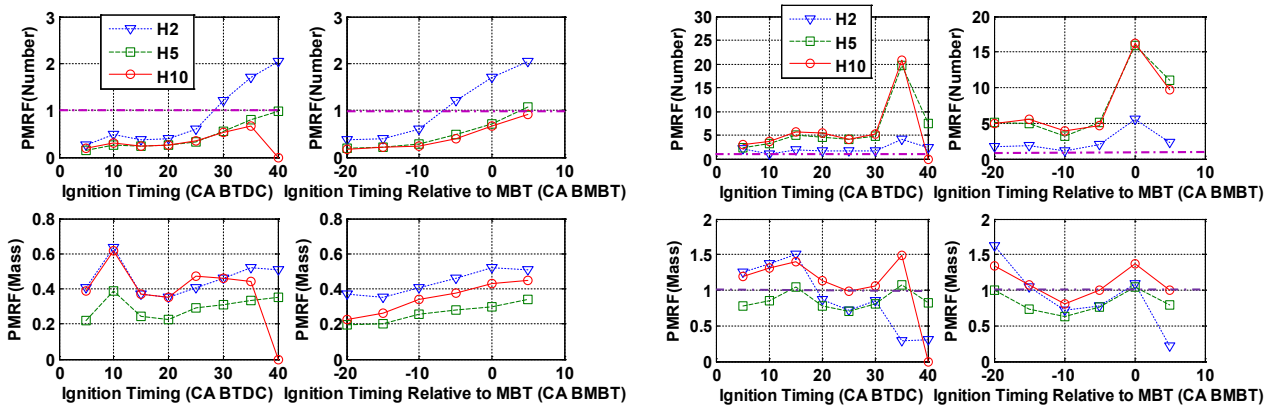

Fig. 10 PMRF (Particulate Matter Reduction Factor) at high load. Left is for λ = 1, right is for λ = 0.9; the train dotted centreline represents PMRF = 1.

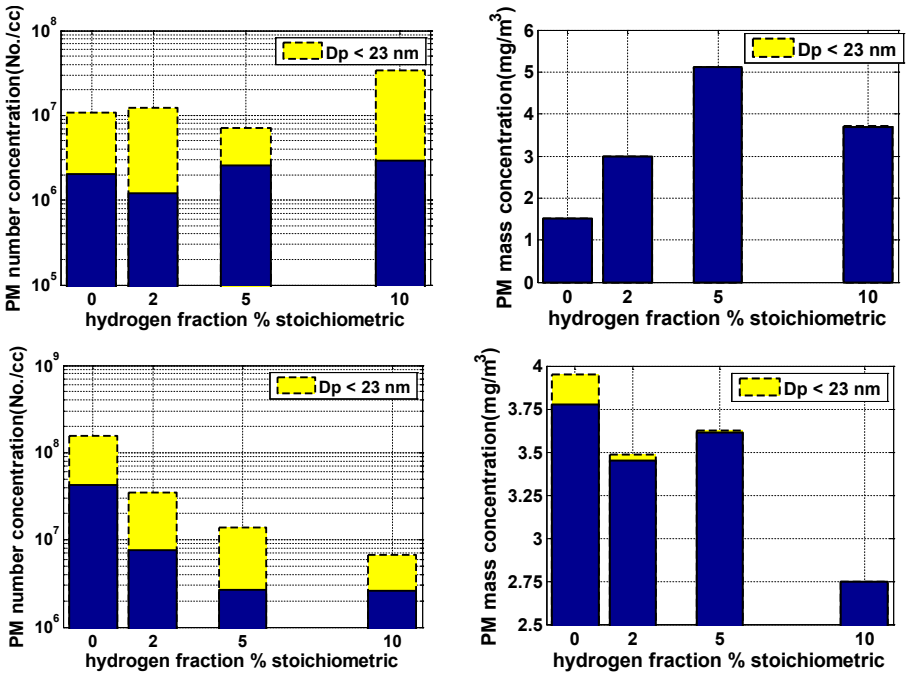

Fig. 11 PM number and mass at the MBT ignition timing at the high load. Upper two figures are for λ = 1, and the lower two are for λ = 0.9.

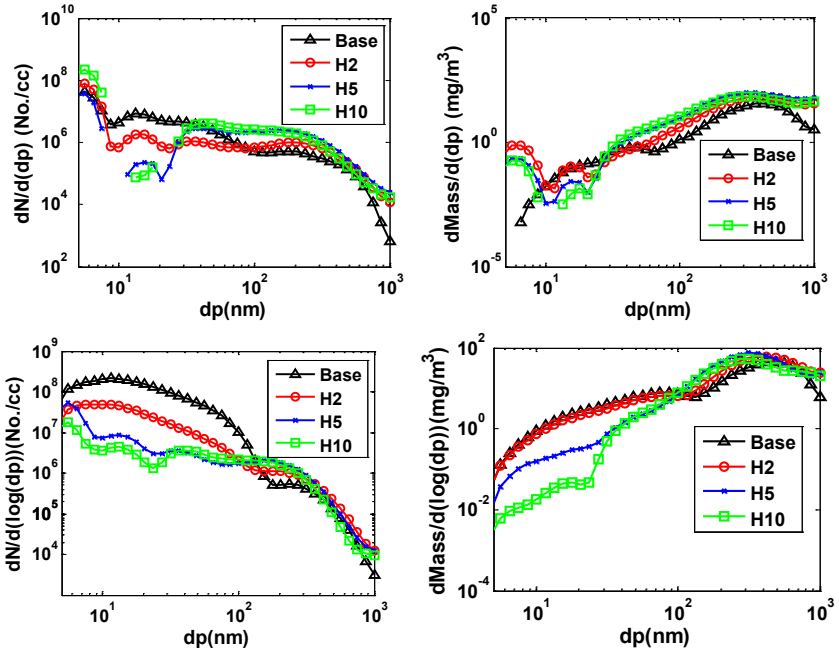

Fig. 12 PM number and mass distribution at MBT ignition timing at high load. Upper two figures are for λ = 1, and the lower two are for λ = 0.9.